Compton scattering studies of Mn-rich Ni-Mn-Ga ferromagnetic shape memory alloys

B. L. Ahuja,[1,*] Gulzar Ahmed,[1] S. Banik,[2] M. Itou,[3] Y. Sakurai,[3] and S. R. Barman[2]
[1]*Department of Physics, University College of Science, M. L. Sukhadia University, Udaipur 313001, India*
[2]*UGC-DAE Consortium for Scientific Research, Khandwa Road, Indore 452017, India*
[3]*Experimental Research Division, Japan Synchrotron Radiation Research Institute, SPring8, Mikazuki, Hyogo 679-5198, Japan*
(Received 28 December 2008; revised manuscript received 21 April 2009; published 5 June 2009)

We report the spin-dependent electron momentum distribution in Mn excess Ni-Mn-Ga ferromagnetic shape memory alloys including Mn_2NiGa using 176.8 keV circularly polarized synchrotron radiation at SPring8, Japan. The magnetic Compton profiles (MCP) were measured at various temperatures and magnetic fields. The data have been analyzed in terms of Mn 3*d*, Ni 3*d* and delocalized spin moments. The magnetic-moment values obtained from the MCP and the behavior of the magnetic effect *R* with temperature and field for the different specimens are in good agreement with our magnetization measurements.

DOI: 10.1103/PhysRevB.79.214403 PACS number(s): 75.25.+z, 75.50.Cc, 83.85.Hf

I. INTRODUCTION

During last decade increased interest in the field of spin electronics has intensified the research work on ferromagnetic shape memory alloys (FSMA). A lot of emphasis was given on the investigation of electronic properties and localized magnetic behavior of Ni_2MnGa and also Ni-rich Ni-Mn-Ga system.[1–12] Ni-Mn-Ga alloys with high contents of Mn and low contents of Ni have been rarely studied. Among the Mn-rich Ni-Mn-Ga systems, the recently discovered Mn_2NiGa is ferrimagnetic at room temperature and exhibits large magneto-elastic coupling with field controllable shape memory effect. It also shows a large thermal hysteresis up to 50 K. It is an attractive material for different technological applications because its martensitic start temperature (270 K) is close to room temperature while the Curie temperature is about 590 K. A large change in magnetic behavior is observed for Mn_2NiGa as compared to Ni_2MnGa due to the excess Mn content.[13] A change in the composition of Ni-Mn-Ga or a partial substitution of the constituent atoms affects several properties such as martensitic transformation temperatures, saturation magnetization, and magnetic anisotropy. Liu *et al.*[14,15] have reported the experimental and theoretical studies related to structural, electronic, and magnetic properties of Mn_2NiGa alloy. Using *ab initio* spin-polarized density-functional theory, Barman and Chakrabarti[16] have rectified the results of Liu *et al.*[15] Barman *et al.*[17] have discussed the electronic and magnetic properties of Mn_2NiGa using full-potential linearized augmented plane-wave method (FP-LAPW) method. The authors have observed Fermi-surface (FS) nesting in the martensitic phase along the [110] direction in the majority-spin FS. They have also shown that the Mn_2NiGa is an itinerant ferrimagnet in both the martensitic and austenitic phases.

The charge Compton profile, $J(p_z)$ is the one-dimensional projection of the electron momentum distribution $n(\mathbf{p})$ along the scattering vector,[18,19]

$$J(p_z) = \int\int n(\boldsymbol{p})dp_x dp_y, \tag{1}$$

where p_z denotes the electron momentum along the scattering vector of the photon. The $n(\mathbf{p})$ is the sum of the majority-spin $n_\uparrow(\mathbf{p})$ and minority-spin $n_\downarrow(\mathbf{p})$ components. The $J(p_z)$ can be obtained experimentally from the energy distribution of the inelastically scattered photons. If the photon impinging on a sample has a component of circular polarization then a spin-dependent term appears in the scattering cross section.[19–21] The Compton profile from unpaired electrons is called magnetic Compton profile (MCP) $J_{\mathrm{mag}}(p_z)$. The $J_{\mathrm{mag}}(p_z)$ is defined as

$$J_{\mathrm{mag}}(p_z) = \int\int [n_\uparrow(\mathbf{p}) - n_\downarrow(\mathbf{p})]dp_x dp_y. \tag{2}$$

Therefore, the MCP reflects the wave functions of the electrons associated with a magnetic ordering. The area under the $J_{\mathrm{mag}}(p_z)$ is equal to the number of unpaired electrons, i.e., the total spin moment per formula unit in Bohr magnetons. Mathematically,

$$\int_{-\infty}^{+\infty} J_{\mathrm{mag}}(p_z)dp_z = \mu_{\mathrm{spin}}. \tag{3}$$

In such measurements, p_z is expressed in atomic units (a.u.), where 1 a.u. $=1.99\times10^{-24}$ kg m s^{-1}. The magnetic Compton scattering (MCS) is a uniquely sensitive probe to find out the magnetic properties in ferrimagnetic and ferromagnetic compounds. In the MCS experiments one also obtains information about the magnetic effect (R), which is proportional to the magnitude of total spin moment in magnetic-ordered states. The R is written as

$$R = \frac{I^+ - I^-}{I^+ + I^-} \propto \mu_{\mathrm{spin}}, \tag{4}$$

where I^+ and I^- are the intensities of scattered photons for the magnetization being parallel and antiparallel to scattering vector, respectively. The sign of the magnetic effect shows the direction of the total spin moment.

To shed more light on temperature and field-dependent magnetism of Mn-rich Ni-Mn-Ga ferromagnetic shape memory alloys, in this paper, we report a systematic study of spin-momentum density using Compton scattering technique. We have undertaken the first-ever magnetic Compton measurements at SPring8, Japan with a view to study the

magnetic Compton profiles at various temperatures (ranging between 50 K and room temperature) and external magnetic fields (0.1–2.5 T) and compare with magnetization measurements and available FP-LAPW calculations.

II. EXPERIMENT

The MCP measurements were performed using a magnetic Compton spectrometer available at BL08W beamline in SPring8.[21] The incident x rays (elliptically polarized) of energy 176.8 keV were selected using a Johann-type Si (620) monochromator. The beam size at the sample position was limited by slits and was 0.5 mm (h)$\times$0.5 mm (w). The overall momentum resolution [Gaussian, full width at half maximum (FWHM)] of spectrometer, which was mainly restricted by an energy resolution of the Ge detectors, was 0.40 a.u. The detection system, which was used to analyze the energy spectra of Compton-scattered synchrotron radiations, consisted of ten Ge elements with individual spectroscopy amplifiers, analog-to-digital converters, and multichannel analyzers. The multiarray Ge crystals (100 mm^2 cross section) were circularly arranged around a hole (11 mm diameter) to collect the scattered photons. The distance between the detector and sample was 1 m. The usual data-reduction procedures for the energy dependence of the detector efficiency, absorption, and the relativistic scattering cross-section corrections were applied. The correction for the multiple scattering was neglected, as the spin-dependent multiple scattering is always very small.[22,23] The data were then converted from energy to momentum scale. Since $J_{mag}(p_z)$ were symmetric about the p_z=0, the profiles were folded leading to a reduction in error bars by a factor of $\sqrt{2}$. The temperature of the sample was changed using a two-stage Gifford-McMohan-type refrigerator operating with He gas circulation. It was attached to a superconducting magnet, which was used to vary the magnetic field up to $\pm$2.5 T during the present measurements. The magnetic field in the sample was flipped parallel (A) and antiparallel (B) to the scattering vector in the sequence of *ABBAABBA*..... The counting time in each position was 60 s with a 6 s interval to ramp the field. Finally, the magnetic profiles were normalized to a spin moment per formula unit with reference to the calibration measurements on Fe as discussed in our earlier work on Ni_2MnGa.[23]

The samples were prepared by melting the constituent metals in correct proportion in arc furnace and subsequent annealing. The details are provided in Refs. 17 and 24. The composition was determined by energy dispersive analysis of x rays (EDAX). The magnetization measurements were carried out using an indigenous vibrating sample magnetometer (VSM) Ref. 25 and a PPMS-VSM (14 T physical property measurement system-vibrating sample magnetometer, M/s Quantum Design, USA) in the temperature range 10–300 K.

III. RESULTS AND DISCUSSION

The martensitic transition temperatures of the different Mn excess Ni-Mn-Ga specimens studied here have been determined by magnetization measurement at low fields and differential scanning calorimetry (DSC) (Fig. 1). A decrease in magnetization in presence of small magnetic field is observed due to the large magnetocrystalline anisotropy in the martensitic phase.[26] From Fig. 1, the martensitic start temperature (M_S) for $NiMn_2Ga$ (or Mn_2NiGa, as we will henceforth call it to be consistent with previous literature), $Ni_{1.75}Mn_{1.25}Ga$, and $Ni_{1.84}Mn_{1.17}Ga$ are determined to be 272, 67, and 137 K, respectively, from the cooling-cycle data of magnetization and DSC and are indicated by the ticks in Fig. 1. These values are in agreement with literature.[14] The hysteresis shown by the heating and cooling cycles in Fig. 1 is the characteristic of the first-order nature of the martensitic transition. It may be noted that the $M(T)$ behavior in high field is different from the low field, as shown in Fig. 1 for $Ni_{1.75}Mn_{1.25}Ga$. Here, the magnetization (which is close to saturation and hence the magnetocrystalline anisotropy effect observed in low field is not visible) increases in the martensitic phase. This increase is intrinsic and is due to higher saturation magnetization in the martensitic phase, which results from the alterations in interatomic bonding related to the change in structure.[24]

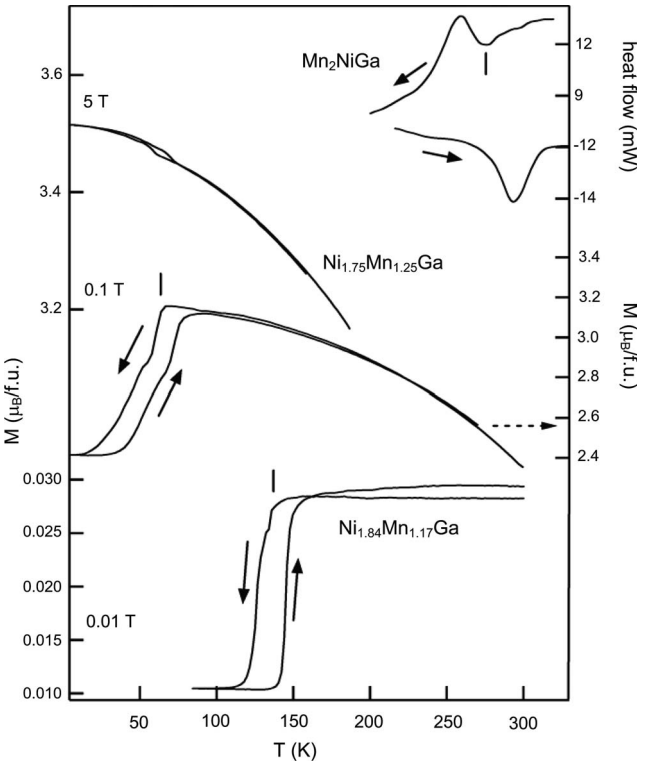

FIG. 1. Magnetization as a function of temperature at low and high fields and differential scanning calorimetry for different Mn excess Ni-Mn-Ga specimens.

The variation in R with temperature and magnetic field for Mn_2NiGa, $Ni_{1.75}$ $Mn_{1.25}Ga$, and $Ni_{1.84}Mn_{1.17}Ga$ are shown in Fig. 2. In Fig. 2(a), in presence of high magnetic field (2.5 T), R exhibits an increase toward lower temperature in $Ni_{1.84}Mn_{1.17}Ga$, which is the expected behavior of magnetization for a ferromagnet. Our data for Mn_2NiGa (also shown in an expanded scale in the inset of [Fig. 2(a)], depicts an increase in magnetization across the martensitic transition around 270 K. Figure 2 further shows that both

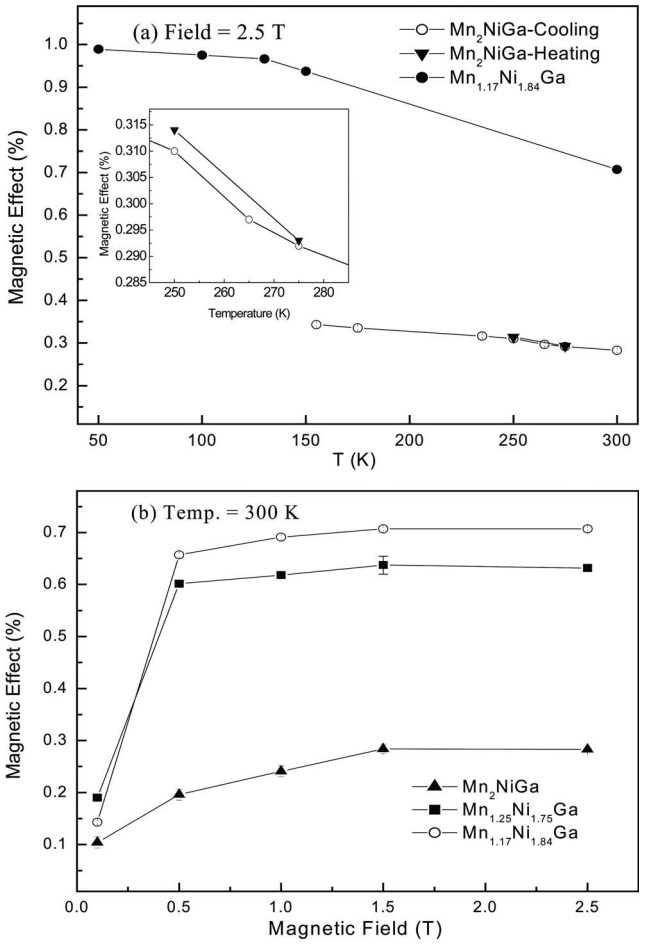

FIG. 2. (a) Variation in magnetic effect (r) in $NiMn_2Ga$ (or Mn_2NiGa) and $Ni_{1.84}Mn_{1.17}Ga$ with temperature at a fixed field 2.5 T (b) Variation in magnetic effect (R) in Mn_2NiGa, $Ni_{1.75}Mn_{1.25}Ga$ and $Ni_{1.84}Mn_{1.17}Ga$ with magnetic field at room temperature (300 K).

$Ni_{1.84}Mn_{1.17}Ga$ and $Ni_{1.75}Mn_{1.25}Ga$ have higher R (and hence higher magnetic moment) in comparison to Mn_2NiGa. This is in agreement with magnetization measurements for Mn excess Ni-Mn-Ga.[14] This is explained by theoretical calculations in terms of an antiparallel configuration of the excess Mn atoms that decreases the total saturation moment for specimens with higher Mn doping.[17,27] Thus, for higher Mn-doped samples, a decrease in the magnetic effect is expected. Another point to be noted is that at 300 K, $Ni_{1.75}Mn_{1.25}Ga$ and $Ni_{1.84}$ $Mn_{1.17}Ga$ are in the austenitic phase and hence R tends to saturate at a lower magnetic field (0.5 T) [Fig. 2(b)]. On the other hand, Mn_2NiGa has a sizable fraction of martensitic phase at room temperature this is evident from the DSC data in Fig. 1. As mentioned earlier, this shows that the martensitic phase has high magnetocrystalline anisotropy and hence the saturation field is expected to be higher. The R variation in Mn_2NiGa can be related to this: it tends to saturate at a higher field of about 1.5 T compared to that of the other specimens that are in the austenitic phase at room temperature.

The experimental $J_{mag}(p_z)$ for Mn-rich alloys at different temperatures and fields (normalized to total spin moments)

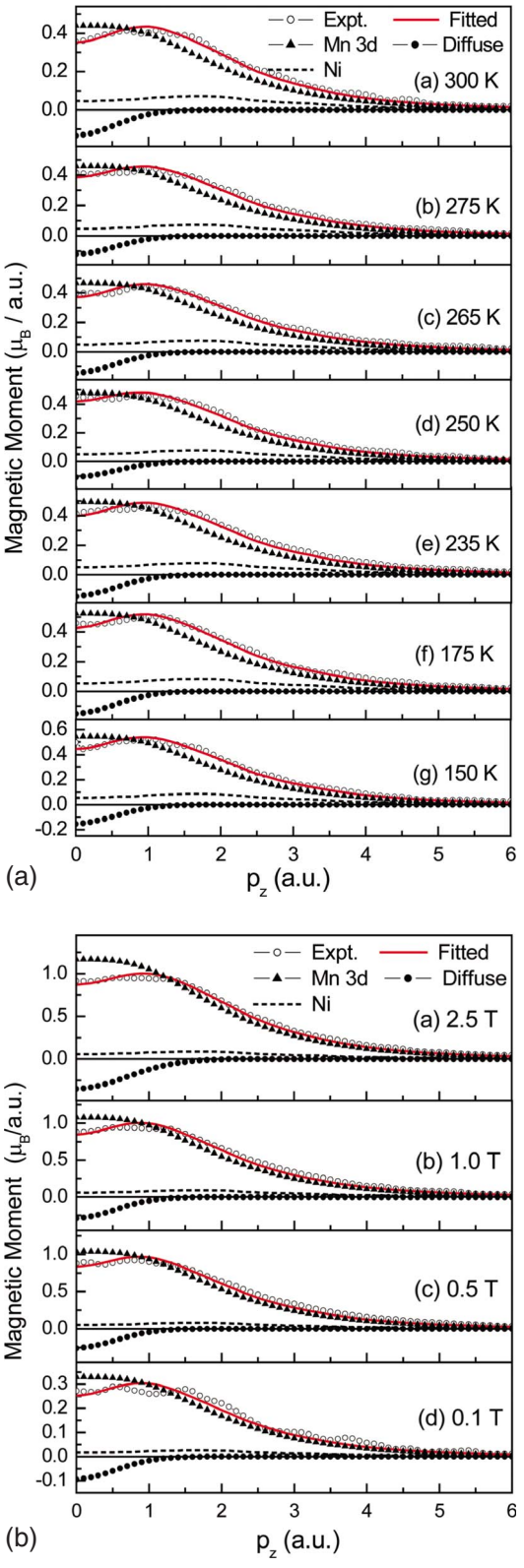

FIG. 3. (Color online) Spin-polarized momentum distribution of (a) Mn_2NiGa at fixed 2.5 T field and different temperatures (b) $Ni_{1.75}Mn_{1.25}Ga$ at room temperature and different fields decomposed into the Mn 3d, Ni (magnetic, fixed), and diffuse components. The total best-fit curve is shown as a solid line through the data points. Statistical error in MCP data is within the size of symbols used.

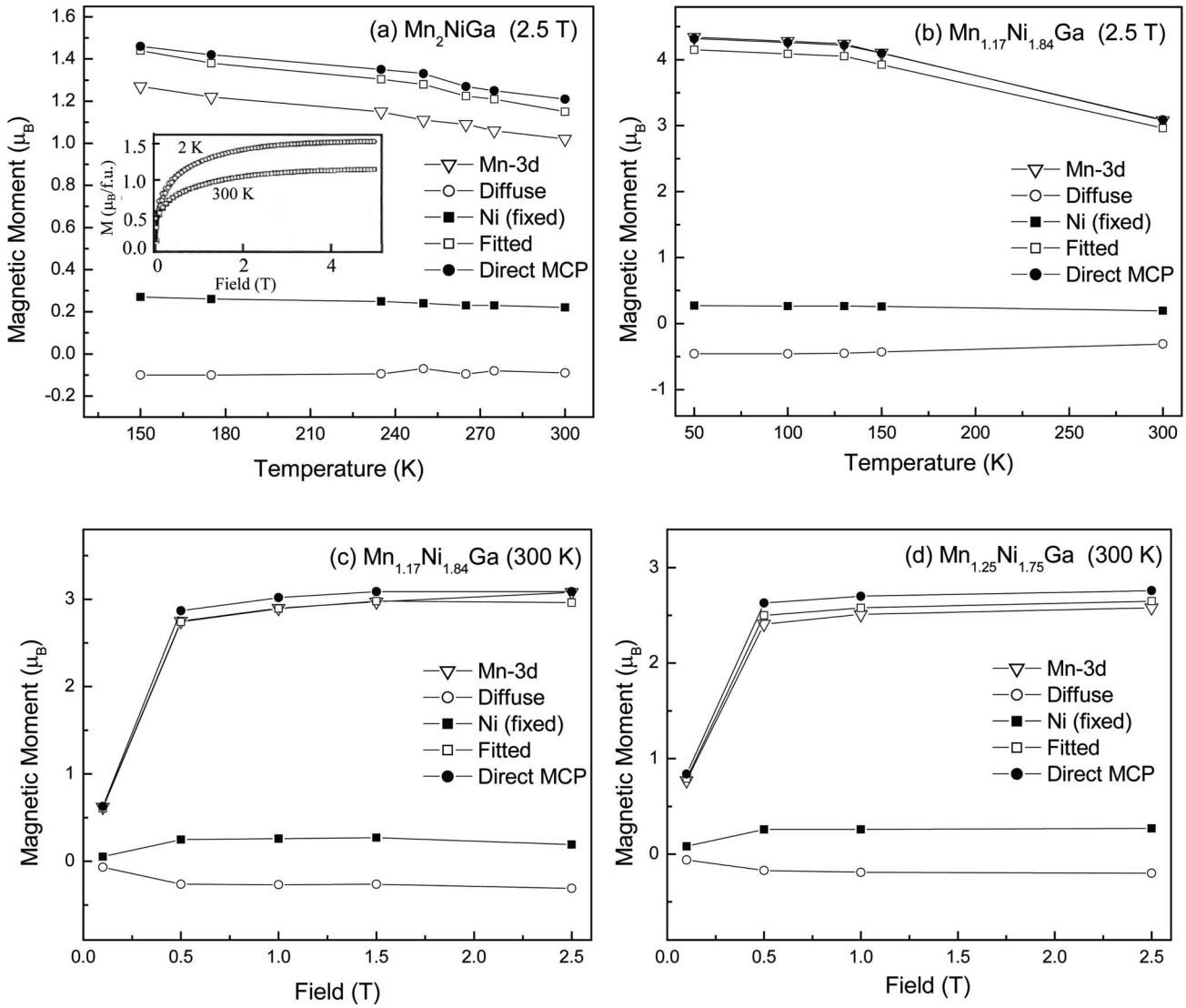

FIG. 4. Temperature and field-dependent magnetic moments determined by the line-shape analysis of the magnetic Compton profiles of (a) Mn_2NiGa at 2.5 T, (b) $Ni_{1.84}Mn_{1.17}Ga$ at 2.5 T, (c) $Ni_{1.84}Mn_{1.17}Ga$ at 300 K, and (d) $Ni_{1.75}Mn_{1.25}Ga$ at 300 K. The error at Mn site is within the size of symbols used. The spin moment per formula unit (μ_B) is equal to the area under the component curves as shown in Fig. 3. The inset shows the isothermal magnetization as a function of field at 2 and 300 K

are shown in Fig. 3. These profiles can be split into relative contribution from the different atomic sites using the Compton profiles calculated using the free-atom basis functions.[28] This approach has been found to be successful in a number of rare-earth compounds[19,22] and our recent data on Ni_2MnGa.[23]

In case of Ni-Mn-Ga, the free-atom Compton profiles of Ni (3*d*) and Mn (3*d*) are almost similar at the present experimental resolution. Therefore, it is difficult to split the total $J_{mag}(p_z)$ in Ni 3*d* and Mn 3*d* components. To overcome this situation, we have taken the fixed contribution of Ni, as in our earlier work.[23] To a good approximation, for the highest field and the lowest temperature, the Ni spin moment was assumed to be $0.27\mu_B$ as obtained from FP-LAPW calculations.[17] As functions of field and temperature, the Ni contribution was varied in proportion to the experimentally determined total magnetic moment. To incorporate the magnetic contribution of Ni, we have taken the spherical average of the local spin-density-based magnetic Compton profile of Ni.[29] For the diffuse components; the free-electron Compton profile was taken as

$$J(p_z) = \begin{cases} \dfrac{3n}{4p_F^3}(p_F^2 - p_z^2) & \text{for } p_z < p_F \quad (p_F = \text{Fermi momentum}) \\ 0 & \text{for } p_z \geq p_F. \end{cases} \tag{5}$$

Therefore, an inverted parabola like free-electron Compton profile is built up by slices through the Fermi sphere of radius p_F in the momentum space.[19] To model the contribution of the diffuse components (Mn 4*s* and Ga 4*s*, 4*p* and 3*d*), we have used the FWHM of the free-electron profile and derived an equivalent Gaussian profile. Before fitting the theoretical profiles corresponding to Mn 3*d*, Ni 3*d* and diffuse contribu-

tions to the experimental data, all the theoretical line shapes have been convoluted by a Gaussian FWHM of 0.40 a.u. It may be noted that the convolution incorporates the effect of instrumental broadening in the theoretical data and plays a significant role in the fitting process. The decomposition of the magnetic profiles at different temperatures and magnetic fields for Mn_2NiGa and $Ni_{1.75}Mn_{1.25}Ga$, respectively, are shown in Figs. 3(a) and 3(b).

In Figs. 4(a)–4(d), the total spin moments along with site-dependent moments are plotted. In case of Mn_2NiGa, the contribution of the total and decomposed magnetic moment decreases slowly with the temperature. The total spin moment mainly arises from Ni and Mn 3*d*. From our MCP data [Fig. 4(a)], the spin magnetic moment at 155 K (lowest temperature taken) and 2.5 T is about $1.46\mu_B$. It is in good agreement with the *M-H* data shown in the inset of Fig. 4(a), at 2 and 300 K, the magnetic moment in presence of 2.5 T field is about 1.5 and $1.1\mu_B$, respectively. For $Ni_{1.84}Mn_{1.17}Ga$, the diffuse and Ni contributions almost cancel each other and the total spin moment is dominated by the Mn 3*d* contribution. A dominant character of Mn 3*d* spin moment is also seen at 300 K in both the fractional compositions of Mn-rich Ni-Mn-Ga system. The MCP data for $Ni_{1.75}Mn_{1.25}Ga$ shows the saturation of the total spin magnetic moment at about 1 T. From the direct MCP data, it is found to be about $2.6\mu_B$. It is in good agreement with our recently published *M-H* data ($2.62\mu_B$ at 283 K).[24] The good agreement between the MCP data that measures only the spin moment and the magnetization indicates that the contribution from orbital moment is small in Mn excess Ni-Mn-Ga, and similar result has been obtained earlier for Ni excess Ni-Mn-Ga.[23] It is worthwhile to mention here that the total spin moment does not depend on the single or polycrystalline nature of the magnetic material.

IV. CONCLUSIONS

The magnetic Compton profiles of Mn-rich Ni-Mn-Ga systems at different temperatures have been analyzed to study the magnetic transitions in terms of spin-moment contribution of Mn 3*d*. The total spin moments are in agreement with the magnetization measurements. The behavior of magnetic effect *R* with field and temperature has been explained by the magnetization studies. The present work also demonstrates that there is a small contribution of the orbital magnetic moment in Mn-rich Ni-Mn-Ga system.

ACKNOWLEDGMENTS

The work at SPring8 was performed with the approval of Japan Synchrotron Radiation Research Institute (JASRI) under Proposal No. 2007B-1065. B. L. Ahuja and G. Ahmed are grateful to DST, New Delhi and A. K. Raychaudhuri for travel support to visit SPring8, Japan. A. M. Awasthi, P. L. Paulose, D. M. Phase are thanked for support. S.B. and S.R.B. acknowledge the funding from Ramanna Research Grant. DST, New Delhi is acknowledged for funding the 14 T-PPMS-VSM at CSR, Indore.

*blahuja@yahoo.com

[1] A. N. Vasil'ev, A. D. Bozhko, V. V. Khovailo, I. E. Dikshtein, V. G. Shavrov, V. D. Buchelnikov, M. Matsumoto, S. Suzuki, T. Takagi, and J. Tani, Phys. Rev. B **59**, 1113 (1999).
[2] A. Ayuela, J. Enkovaara, K. Ullakko, and R. M. Nieminen, J. Phys.: Condens. Matter **11**, 2017 (1999).
[3] S. J. Murray, M. Marioni, S. M. Allen, R. C. O'Handley, and T. A. Lograsso, Appl. Phys. Lett. **77**, 886 (2000).
[4] A. Sozinov, A. A. Likhachev, N. Lanska, and K. Ullakko, Appl. Phys. Lett. **80**, 1746 (2002).
[5] Y. Lee, J. Y. Rhee, and B. N. Harmon, Phys. Rev. B **66**, 054424 (2002).
[6] C. Biswas, R. Rawat, and S. R. Barman, Appl. Phys. Lett. **86**, 202508 (2005).
[7] V. V. Khovailo, V. Novosad, T. Takagi, D. A. Filippov, R. Z. Levitin, and A. N. Vasil'ev, Phys. Rev. B **70**, 174413 (2004).
[8] S. R. Barman, S. Banik, and A. Chakrabarti, Phys. Rev. B **72**, 184410 (2005).
[9] A. Chakrabarti, C. Biswas, S. Banik, R. S. Dhaka, A. K. Shukla, and S. R. Barman, Phys. Rev. B **72**, 073103 (2005).
[10] S. Banik, A. Chakrabarti, U. Kumar, P. K. Mukhopadhyay, A. M. Awasthi, R. Ranjan, J. Schneider, B. L. Ahuja, and S. R. Barman, Phys. Rev. B **74**, 085110 (2006).
[11] C. P. Opeil, B. Mihaila, R. K. Schulze, L. Manosa, A. Planes, W. L. Hults, R. A. Fisher, P. S. Riseborough, P. B. Littlewood, J. L. Smith, and J. C. Lashley, Phys. Rev. Lett. **100**, 165703 (2008).
[12] M. A. Uijttewaal, T. Hickel, J. Neugebauer, M. E. Gruner, and P. Entel, Phys. Rev. Lett. **102**, 035702 (2009).
[13] F. Albertini, A. Paoluzi, L. Pareti, M. Solzi, L. Righi, E. Villa, S. Besseghini, and F. Passaretti, J. Appl. Phys. **100**, 023908 (2006).
[14] G. D. Liu, J. L. Chen, Z. H. Liu, X. F. Dai, G. H. Wu, B. Zhang, and X. X. Zhang, Appl. Phys. Lett. **87**, 262504 (2005).
[15] G. D. Liu, X. F. Dai, S. Y. Yu, Z. Y. Zhu, J. L. Chen, G. H. Wu, H. Zhu, and J. Q. Xiao, Phys. Rev. B **74**, 054435 (2006).
[16] S. R. Barman and A. Chakrabarti, Phys. Rev. B **77**, 176401 (2008).
[17] S. R. Barman, S. Banik, A. K. Shukla, C. Kamal, and A. Chakrabarti, Europhys. Lett. **80**, 57002 (2007).
[18] *Compton Scattering*, edited by B. Williams (McGraw-Hill, New York, 1977).
[19] *X-ray Compton Scattering*, edited by M. J. Cooper, P. E. Mijnarends, N. Shiotani, N. Sakai, and A. Bansil (Oxford University Press, Oxford, 2004); W. Schulke *Electron Dynamics by Inelastic X-Ray Scattering* (Oxford University Press, Oxford, 2007).
[20] N. Sakai, J. Appl. Crystallogr. **29**, 81 (1996).
[21] B. L. Ahuja, Vinit Sharma, and Y. Sakurai, Adv. Mater. Res. **52**, 145 (2008), and references therein; Y. Kakutani, Y. Kubo, A. Koizumi, N. Sakai, B. L. Ahuja, and B. K. Sharma, J. Phys. Soc. Jpn. **72**, 599 (2003).
[22] B. L. Ahuja, T. Ramesh, B. K. Sharma, P. Chaddah, S. B. Roy, Y.

Kakutani, A. Koizumi, N. Hiraoka, M. Toutani, N. Sakai, Y. Sakurai, and M. Itou, Phys. Rev. B **66**, 012411 (2002).
[23] B. L. Ahuja, B. K. Sharma, S. Mathur, N. L. Heda, M. Itou, A. Andrejczuk, Y. Sakurai, A. Chakrabarti, S. Banik, A. M. Awasthi, and S. R. Barman, Phys. Rev. B **75**, 134403 (2007).
[24] S. Banik, R. Rawat, P. K. Mukhopadhyay, B. L. Ahuja, Aparna Chakrabarti, P. L. Paulose, Sanjay Singh, Akhilesh Kumar Singh, D. Pandey and S. R. Barman, Phys. Rev. B **77**, 224417 (2008).
[25] R. V. Krishnan and A. Banerjee, Rev. Sci. Instrum. **70**, 85 (1999).
[26] F. Albertini, L. Pareti, A. Paoluzi, L. Morellon, P. A. Algarabel, M. R. Ibarra, and L. Righi, Appl. Phys. Lett. **81**, 4032 (2002).
[27] J. Enkovaara, O. Heczko, A. Ayuela, and R. M. Nieminen, Phys. Rev. B **67**, 212405 (2003).
[28] F. Biggs, L. B. Mandelsohn, and J. B. Mann, At. Data Nucl. Data Tables **16**, 201 (1975).
[29] M. A. G. Dixon, J. A. Duffy, S. Gardelis, J. E. McCarthy, M. J. Cooper, S. B. Dugdale, T. Jarlborg, and D. N. Timms, J. Phys.: Condens. Matter **10**, 2759 (1998).